Elastic energy propagation in a strongly scattering 1D laboratory model

Kasper van Wijk, Matthew Haney and John A. Scales
Center for Wave Phenomena and Physical Acoustics Laboratory, Colorado School of Mines

ABSTRACT
Laboratory ultrasonics provides an ideal opportunity for studying wave propagation in random media. Models are relatively easy to construct and both the phase and amplitude of the wave field can be measured, so we can separate the coherent from the incoherent intensity. Here we show detailed measurements of wave propagation in a 1D strongly scattering medium that fit the theory of radiative transfer for both short times (ballistic propagation) and long times (diffusive propagation). Including late time information gives us a unique opportunity to separate scattering attenuation from intrinsic absorption.

INTRODUCTION

When waves propagate through a medium they encode information about the properties of that medium. The information encoded by multiply scattered waves has a very different character than that associated with directly propagating or singly-scattering waves. Consider two examples. A normal mode or standing wave can be thought of as the superposition of traveling waves that repeatedly sample a finite medium (by reflection from or propagation around boundaries). Thus small changes in the size or properties of the medium are amplified by each pass of the traveling waves; this amplification leads to the exquisite precision of spectroscopy, allowing one to infer properties that would be completely undetectable with directly propagating waves (Zadler *et al.*, 2003). On the other hand, suppose a wave passes through a cloud of similar scatterers; if some property of the scatterers changes, then this effect is repeatedly imparted on the multiply-scattered wave, making it potentially observable even when the perturbation of a single scatterer is unresolvable (Snieder *et al.*, 2002; Lemieux *et al.*, 1998; Cowan *et al.*, 2002).

In practice, however, exploiting multiply scattered waves to make inferences about a medium can be far more complicated than using single-scattering theory such as the Born approximation. In seismology, for example, nearly all data processing algorithms are based on single scattering theory (Aki & Richards, 1980). In optics, there has been growing interest in using effective medium theories such as radiative transfer to model the transport of energy in random media (Lemieux *et al.*, 1998). It is in these cases of strong scattering where phases are randomized, that the single scattering model loses its relevance. In geophysics, the scattering medium can be a highly heterogeneous near-surface (Campman *et al.*, 2003), crust (Campillo *et al.*, 1999), or the rough boundary between core and mantle (Earle & Shearer, 1997), while in medical imaging tissue is such a strong scatterer of light, that only diffuse (i.e., multiply scattered) light samples the target (Boas *et al.*, 1995).

In seismology and laboratory ultrasonics, we have the advantage of being able to measure both the amplitude and phase of the wave field. Nevertheless, radiative transfer models provide the opportunity to extract information about the mean free scattering and absorption lengths as well as the diffusion constant. At early times the energy propagates ballistically, while at later times it propagates diffusively. Beautiful examples of this transition can be seen in the propagation of bulk phonons at low temperature (Narayanamurti *et al.*, 1978), while time-resolved images of this transition in random media such as rocks have been presented in (Scales & Malcolm, 2003).

To study the propagation of strongly scattering surface waves in the Physical Acoustics Laboratory (PAL), the solution to the radiative transfer equation in 1D (Haney *et al.*, 2003) is used to describe the data with parameters such as scattering strength, attenuation and energy velocity. Even though formally speaking, energy is localized in 1D random media, our data and theory (Sheng, 1995, equation (6.41)) suggest there is a window where energy behaves diffusively, and the radiative transfer model is valid. In this window it is possible to separate scattering attenuation from intrinsic absorption. With the latter an indicator of fluids, this

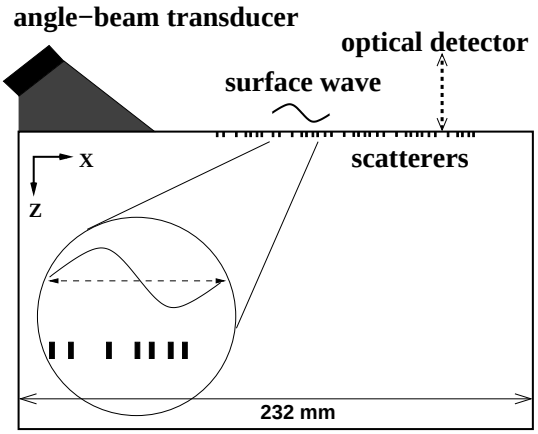

Figure 1. Side-view of the angle-beam transducer launching nearly-plane surface waves into the grooved aluminum block.

method is potentially of great interest for exploration geophysics.

1 EXPERIMENTAL CONFIGURATION

The setup of our experiment is shown in Figure 1. A 200 V repetitive pulse is used to excite an angle-beam transducer mounted on the surface of a grooved aluminum block of dimensions 28 cm × 23 cm × 21.5 cm. The transducer wedge has a footprint of 7 cm (in the forward direction) by 4.2 cm. The angle of the transducer is such that its output in the aluminum model is almost exclusively a plane surface (Rayleigh) wave.

The aluminum block has a Fibonacci pattern of aligned linear grooves machined into one face. This pattern is quasi-periodic, increasing in complexity as the sequence gets longer (Carpena *et al.*, 1995). The grooves are 1 mm wide by 3 mm deep, while the dominant wavelength of the surface waves is about 15 mm, so there are many scatterers per wavelength as waves propagate perpendicular to the grooves. While plane waves are incident at right angles on grooves that extend over the entire length of the model, consistent with a 1D model, surface wave energy is lost to body wave diffractions at each groove. We treat this diffracted energy as attenuation (i.e., loss) in a 1D medium; intrinsic absorption in the aluminum is virtually zero.

The wave field is detected using a scanning laser interferometer that measures absolute particle velocity on the surface of the sample via the Doppler shift. The signal was digitized at 14-bit resolution using a Gage digital oscilloscope card attached to a PC. This setup allows us to measure multiply-scattered waves between the scatterers (i.e. *inside* the scattering medium).

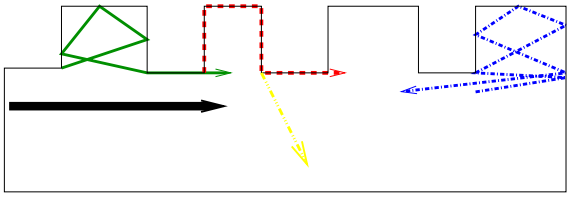

Figure 2. Side-view of paths for (scattered) rays in grooved aluminum: some surface waves travel undisturbed under the grooves, others follow the contours of the grooves, and again others are diffracted to body waves.

2 RADIATIVE TRANSFER OF ENERGY

The radiative transfer equation can be derived from the ladder approximation to the Bethe-Salpeter equation (van Rossum & Nieuwenhuizen, 1999), and is used to describe the intensity in strongly scattering media. Often this model is intuitively explained by a random walk of photons or phonons between scatterers in a homogeneous background material (Paasschens, 1997; Lemieux *et al.*, 1998). In our experiment, the behavior of scattering surface waves is complex (Viktorov, 1967), but the "random walk" includes the paths in Figure 2.

The Green's function for the 1D radiative transfer equation with attenuation and a directional source is (Haney *et al.*, 2003):

$$G(x,t) \propto e^{-vt(R/l_s+1/l_a)} \left[2\delta\left(\frac{l_s}{R}(x-vt)\right) + u(vt-|x|)\left(I_0(\eta) + \sqrt{\frac{vt+x}{vt-x}} I_1(\eta)\right)\right]. \quad (1)$$

The argument of the Modified Bessel functions of order zero (I_0) and one (I_1) is

$$\eta = \frac{R}{l_s}\sqrt{(vt)^2 - x^2},$$

where v is the energy velocity and u the step function to assure causality in the system. The energy losses to body wave diffractions at the grooves are modeled by the attenuation term l_a. R is the backscattering cross-section for a single groove and l_s is the scattering mean free path. Note that R and l_s are coupled, so they cannot be resolved individually from expression (1).

The term with the Dirac delta function represents the ballistic propagation of energy, or the coherent signal, from here on denoted as $C(x,t)$, while the Bessel functions describe the incoherent signal $I(x,t)$. Both terms decay exponentially depending on attenuation (in our case body-wave diffraction) and scattering; the latter being a redirection of energy due to scattering. For large times ($vt >> x$) the coherent energy is zero and the incoherent signal simplifies to the diffusion equation used to model the data in (Scales & van Wijk, 2001).

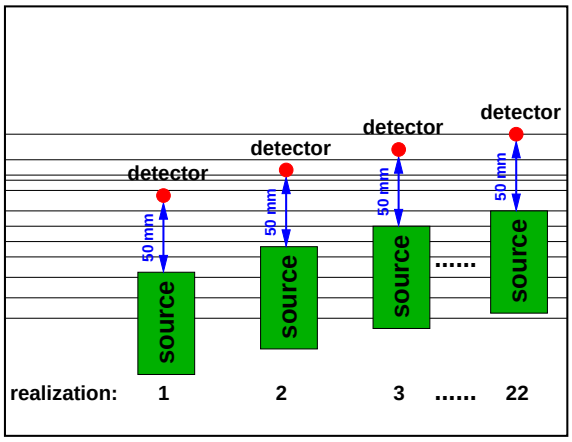

Figure 3. Top-view of the procedure to obtain an ensemble average.

3 OBSERVATIONS

To obtain ensemble measurements over the disordered medium, particle velocity measurements at fixed source-detector distances are collected for different positions in the groove sequence (Figure 3). We used three sets of 22 realizations with the detector 25, 50 and 75 mm from the leading edge of the source. Figure 4 contains waveforms recorded at 50 mm source-detector spacing. The left panel shows particle velocity for the 22 source-detector locations in the ensemble measurement. Around 0.025 ms all traces contain relatively large amplitudes that are in phase. This is the coherent signal. This part of the signal is independent of local variations in the scattering distribution, whereas the later arrivals (also known as "coda") vary in phase and amplitude for each source-detector location. This is the incoherent signal due to scattering from the micro-structure in the medium. These features are even more clear in the average trace in the middle panel of Figure 4: while the incoherent signal tends to average out, the coherent signal is enhanced in the averaging procedure. The right panel contains the ensemble-averaged intensities. The total intensity is the average of each squared particle velocity trace from the left panel, and the coherent intensity is the square of the mean of the particle velocity traces (middle panel). The coherent intensity was smoothed by a running window of width 25 samples to suppress large fluctuations caused by zero crossings intrinsic to the coherent wave forms. By definition, the coherent intensity is less than the total intensity (Ishimaru, 1997).

4 FITTING THE DATA WITH RADIATIVE TRANSFER

We now estimate the scattering and absorption mean free paths and the energy velocity using the radiative transfer equation by fitting the laboratory data. Since we are able to separate both the data and the radiative transfer equation into a coherent and an incoherent part, we will treat the parameter-fitting problem for each part separately. For clarity, we drop scaling terms in the solution to the radiative transfer equation from here on, since all data and simulations are normalized to amplitudes at the first source-detector offset.

The Green's function in expression (1) is convolved with the band-limited input energy pulse. Actually determining the source signal is not trivial; because as the source is moved across the grooves, the source wavelet is not that of the source mounted on the smooth surface of aluminum. Not only is the coupling between the source wedge and the model changed when grooves are present, scattering takes place at the grooves *under* the source wedge, effectively low-pass filtering the source wavelet.

4.1 Coherent intensity

The coherent part $C(x,t)$ of the Green's function of the 1D attenuative radiative transfer equation is:

$$C(x,t) \propto \delta(x - vt)\; e^{-\alpha v t}. \qquad (2)$$

The solid line in Figure 5 is the modeled envelope of the coherent intensity for $\alpha = R/l_s + 1/l_a = 17.8$ m^{-1} and velocity $v = 1818 \pm 123$ m/s. In our case the velocity of the coherent energy equals the transport velocity, even though especially for resonant scattering the velocity of the coherent signal can be significantly higher than the group (transport) velocity (Page *et al.*, 1996; Kuga *et al.*, 1993; van Albada *et al.*, 1991). The energy of the coherent signal travels dispersively. As lower frequency surface waves penetrate the model deeper, they travel for a relatively undisturbed by the scatterers, while higher frequencies are slowed by stronger scattering due to the grooves. We therefore model the energy velocity to be a function of frequency. The smaller, secondary peak in the coherent intensity is not modeled. This peak is most likely a part of the source wavelet, not accounted for in the model.

4.2 Incoherent intensity

The incoherent intensity is the difference between the total and the coherent intensity and is plotted as the dashed curves in Figure 6. The solid lines are the result of modeling the incoherent part $I(x,t)$ of (1):

$$I(x,t) \propto e^{-\alpha v t}\left(I_0(\eta) + \sqrt{\frac{vt+x}{vt-x}}I_1(\eta)\right). \qquad (3)$$

Using the energy velocity of 1818 m/s and $\alpha = 17.8$ m^{-1}, the resulting fits in Figure 6 are for $R/l_s = 11.1$ m^{-1}. We fit the incoherent signal only at intermediate times. At short times the incoherent data are incomplete, and at late times energy comes back into the system from reflections off the back of the model. But

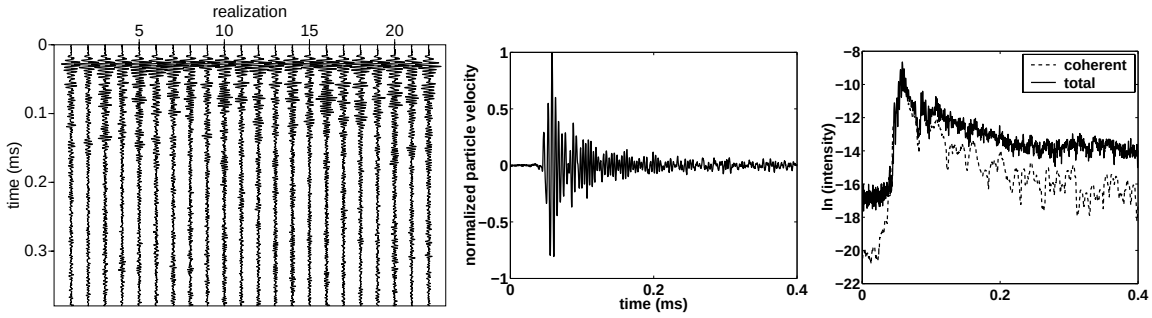

Figure 4. Data at 50 mm source-detector offset. The left panel is particle velocity for 22 realizations, the middle panel the average trace, and the right panel the natural logarithm of the total and coherent intensity.

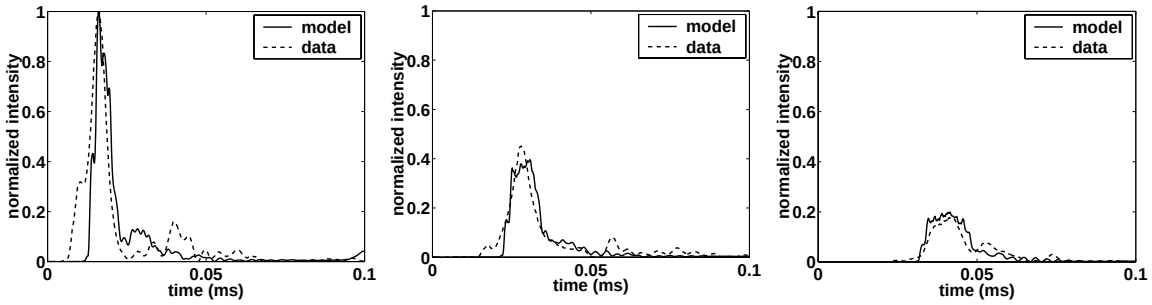

Figure 5. Comparison between the measured and modeled coherent intensities for 25 (left), 50 (middle) and 75 mm (right).

in the intermediate time window, the fit describes the average measured incoherent intensity. Note that the incoherent intensity at intermediate times is of equal amplitude for all three offsets.

4.3 Fitting parameters

With $R/l_s + 1/l_a = 17.8$ m^{-1} and $R/l_s = 11.1$ m^{-1}, the absorption length is $l_a = 0.15$ m. If $R = 0.5$, the mean of the range of possible values, the scattering mean free path is $l_s = 0.05$ m. Data at source-detector offsets around l_s put us in the transitional regime from ballistic to diffusive energy propagation. Formally, these parameters in the radiative transfer are functions of frequency, since our scatterers have a finite depth and surface-wave frequencies sample different depths of the model. The data fit, however, is obtained with an average value for the scattering and absorption parameters. To account for dispersion in the coherent signal, only the energy velocity was treated as a function of frequency.

5 CONCLUSIONS

The strongly scattering surface-wave model presented, shows great flexibility in understanding multiple scattering media. Not only can we measure phase and amplitude of the surface waves (allowing us to separate the coherent from the incoherent signal), we also have the advantage of probing the medium between scatterers. We found that in a region around a mean free path, 1D radiative transfer can describe our scattering medium. Fitting both coherent and incoherent energy allows us to resolve average values for the scattering and absorption mean free paths, effectively separating these causes for attenuation.

ACKNOWLEDGMENTS

The authors thank Roel Snieder, Bart van Tiggelen and everyone in the Physical Acoustics Laboratory for many helpful discussions. This work was supported by the National Science Foundation (EAR-0111804) and the Army Research Office (DAAG55-98-1-0277).

REFERENCES

Aki, K., & Richards, P. G. 1980. *Quantitative seismology: theory and practice.* Freeman.

Boas, D. A., Campbell, L. E., & Yodh, A. G. 1995. Scattering and imaging with diffusing temporal field correlations. *Physical Review Letters*, **75**, 1855–1858.

Campillo, M., Margerin, L., & Shapiro, N. 1999. Seismic wave diffusion in the Earth lithosphere. *Pages 383–404 of:* Fouque, J.-P. (ed), *Diffuse waves in complex media.* Kluwer.

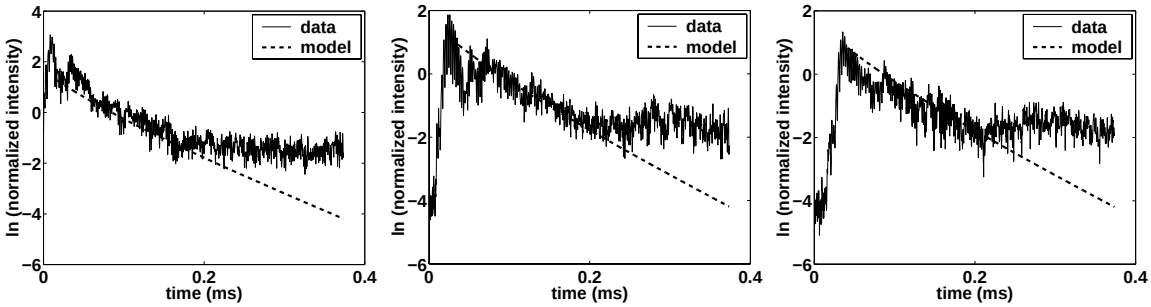

Figure 6. Comparison between the measured and modeled incoherent intensities for 25 (left), 50 (middle) and 75 mm (right).

Campman, X. H., van Wijk, K., Scales, J. A., & Herman, G. C. 2003. Suppression of near-field scattered surface waves. *In: Extended Abstracts, 65th Mtg.* Eur. Assn. Geosci. Eng.

Carpena, P., Gasparian, V., & Ortuño, M. 1995. Energy spectra and level statistics of Fibonacci and Thue-Morse chains. *Physical Review B*, **51**(18), 12813–12816.

Cowan, M. L., Jones, I. P., Page, J. H., & Weitz, D. A. 2002. Diffusing acoustic wave spectroscopy. *Phys. Rev. E*, **65**, 066605.

Earle, P. S., & Shearer, P. M. 1997. Observations of PKKP precursors used to estimate small-scale topography on the core-mantle boundary. *Science*, **277**, 667–670.

Haney, M., van Wijk, K., & Snieder, R. K. 2003. *Radiative Transfer in 1-D attenuative media for non-isotropic scattering.* CWP Project Review.

Ishimaru, A. 1997. *Wave Propagation and Scattering in Random Media.* Oxford University Press.

Kuga, Y., Ishimaru, A., & Rice, D. 1993. Velocity of coherent and incoherent electromagnetic waves in a dense strongly scattering medium. *Phys. Rev. B*, **48**(17), 13155–13158.

Lemieux, P. -A., Vera, M. U., & Durian, D. J. 1998. Diffusing-light spectroscopies beyond the diffusion limit: The role of ballistic transport and anisotropic scattering. *Phys. Rev. E*, **57**(4), 4498–4515.

Narayanamurti, V., Dynes, R. C., Hu, P., Smith, H., & Brinkman, W. F. 1978. Quasiparticle and phonon propagation in bulk, superconducting lead. *Phys. Rev. B.*

Paasschens, J. C. 1997. Solution of the time-dependent Boltzmann equation. *Phys. Rev. E*, **56**, 1135.

Page, J. H., Sheng, P., Schriemer, H. P., Jones, I., Jing, X., & Weitz, D. A. 1996. Group velocity in strongly scattering media. *Science*, **271**(February), 634–637.

Scales, J. A., & Malcolm, A. E. 2003 (April). *Laser characterization of ultrasonic wave propagation in random media.* To appear in Phys. Rev. E.

Scales, J. A., & van Wijk, K. 2001. Tunable multiple-scattering system. *Applied Physics Letters*, **79**, 2294–2296.

Sheng, P. 1995. *Introduction to Wave Scattering, Localization, and Mesoscopic Phenomena.* Academic Press.

Snieder, R., Grêt, A., Douma, H., & Scales, J. A. 2002. Coda Wave Interferometry for Estimating Nonlinear Behavior in Seismic Velocity. *Science*, **295**, 2253–2255.

van Albada, M. P., van Tiggelen, B. A., Lagendijk, A., & Tip, A. 1991. Speed of propagation of Classical Waves in strongly scattering media. *Phys. Rev. Lett.*

van Rossum, M. C. W., & Nieuwenhuizen, Th. M. 1999. Multiple scattering of classical waves: microscopy, mesoscopy, and diffusion. *Reviews of Modern Physics*, **71**(1), 313–371.

Viktorov, I. A. D. 1967. *Rayleigh & Lamb waves. Physical theory and application.* New York: Plenum Press.

Zadler, B., Le Rousseau, J. H. L., Scales, J. A., & Smith, M. L. 2003. Resonant Ultrasound Spectroscopy: theory and application. *CWP Project Review.*